

Impact of Height and Volume on the Seismic Reduction Coefficient for Elevated Tanks in Loreto: A Proposal for the Peruvian Standard E.030

Mirella Alexandra Camarena Verastegui, Gustavo Quispe Paitan, Percy Julio Quispe Paitan, Manuel Ismael Laurencio Luna*

Faculty of Civil Engineering, Continental University, Peru

Received December 9, 2024; Revised February 19, 2025; Accepted March 17, 2025

Cite This Paper in the Following Citation Styles

(a): [1] Mirella Alexandra Camarena Verastegui, Gustavo Quispe Paitan, Percy Julio Quispe Paitan, Manuel Ismael Laurencio Luna, "Impact of Height and Volume on the Seismic Reduction Coefficient for Elevated Tanks in Loreto: A Proposal for the Peruvian Standard E.030," *Civil Engineering and Architecture*, Vol. 13, No. 3, pp. 1624 - 1646, 2025. DOI: 10.13189/cea.2025.130314.

(b): Mirella Alexandra Camarena Verastegui, Gustavo Quispe Paitan, Percy Julio Quispe Paitan, Manuel Ismael Laurencio Luna (2025). *Impact of Height and Volume on the Seismic Reduction Coefficient for Elevated Tanks in Loreto: A Proposal for the Peruvian Standard E.030*. *Civil Engineering and Architecture*, 13(3), 1624 - 1646. DOI: 10.13189/cea.2025.130314.

Copyright©2025 by authors, all rights reserved. Authors agree that this article remains permanently open access under the terms of the Creative Commons Attribution License 4.0 International License

Abstract The Loreto region of Peru faces a severe crisis in access to drinking water, with a large part of the population without adequate supply. Elevated tanks are a common solution, but present significant structural challenges in a seismically active area. The Peruvian standard E.030 does not specify a seismic reduction coefficient (R) for these tanks, leading to the use of foreign standards that do not fit local conditions. This increases the risk of structural failure, especially in inverted pendulum type geometry tanks, which endangers the safety and functionality of the water supply. This study proposes a new equation to estimate the most appropriate seismic reduction coefficient according to the height of the tank, taking into account the seismic conditions in Loreto. Simulations of seismic loads were carried out using the pushover method, evaluating the structural behaviour of 63 elevated tank models. The results show that as the tank height increases, the seismic reduction factor decreases, indicating a lower capacity of the structure to dissipate seismic loads. Models with larger volumes and heights exhibit more plastic behaviour, while smaller and stiffer tanks have lower ductility and reduction factor. The proposed equation, with a linear regression of the form $y = -0.064X + 9.598$, provides an accurate tool to adjust the seismic reduction coefficient as a function of tank height.

This proposal can be incorporated into the E.030 standard, improving the seismic design of elevated tanks in Loreto and other seismically active regions, and reducing the risk of structural failure during seismic events, ensuring a safer and more sustainable water supply.

Keywords Elevated Tanks, Seismic Reduction, Pushover, Creep, Collapse, Ductility, Over Strength

1. Introduction

The water access situation in the Loreto region of Peru is critical. Currently, 43.7% of the population does not have access to drinking water through a public water network or water taps, which highlights the urgency of improving the water infrastructure [1]. In this context, the use of elevated tanks is common in the region, as they guarantee a continuous supply of water 24 hours a day [2], [3], [4]. It should be noted that these structures are considered essential category A buildings, according to Peruvian standard E.030, which establishes strict design, strength and stiffness requirements [5]. However, the design of these tanks faces significant challenges that put

their functionality and safety at risk, especially in rural and urban areas of Loreto. Historically, elevated tanks have demonstrated considerable vulnerability to seismic events. In particular, those supported on column-supported platforms have failed due to container torsion. Additionally, elevated tanks supported on a single column acting as a resisting element have also experienced structural problems [6]. Recent examples include collapses in Mexico in 2022 and 2023, where newly inaugurated structures suffered severe failures resulting in loss of life and property damage [7], [8]. These incidents reveal the problems in the design of elevated tanks, particularly those with complex geometry.

One of the biggest challenges is the lack of a specific seismic reduction coefficient in the Peruvian E.030 standard [5], which forces designers to resort to foreign standards, such as ACI, which establishes coefficients between 2 and 4.75 [9], and FEMA, whose coefficients vary between 2 and 3 [10]. Although useful, these standards are designed for areas with higher seismic demands than Loreto, which may not reflect local needs and may lead to critical structural failures. The use of inappropriate coefficients in seismic design increases the risk of failure in non-ductile structures, which are more prone to brittle failure and sudden collapse during an earthquake event, due to the inability to deform in a controlled manner [11]. In addition, excessive steel reinforcement, without proper distribution of forces, generates unnecessary stresses that compromise tank stability [12], while plastic deformations, which occur when loads exceed the elastic limit of the material, can cause permanent changes that affect its functionality and safety [13], [14]. Material fatigue, produced by repeated loading cycles, accelerates structural deterioration and increases the risk of collapse [15], highlighting the need to develop a specific seismic reduction coefficient for inverted pendulum tanks in Peru.

Addressing design issues and water accessibility is crucial to ensure that the population of Loreto has a safe, efficient and adequate water infrastructure to meet their needs. In this context, the objective of this research is to propose a region-specific seismic design approach that takes into account the local conditions of Loreto. This approach will include the implementation of an adapted seismic reduction coefficient in order to improve the resistance and stability of the elevated tanks to seismic events.

1.1. Literature Review

Over the years, earthquakes have caused severe damage not only to infrastructure such as houses and bridges, but also to elevated water tanks. Figure 1 shows various structural failures in items a, b, c and d. In item a, during the 1960 Chile earthquake with a magnitude of 8.5, a 700 m³ elevated tank suffered a flexural-shear failure of its beams [16]. In item b, corresponding to the 2001 Bhuj,

India earthquake with a magnitude of 7.7, several elevated tanks were severely affected, with deep cracks in their columns, and three of them collapsed completely, with capacities up to 680 m³ [17]. In item c, during the 1997 Jabalpur earthquake, with a magnitude of 5.8, an elevated water tank collapsed completely [18]. Finally, in item d, which shows the 1980 Algeria earthquake with a magnitude of 7.2, an elevated tank failed due to poor detailing of the beam-column connection [16]. These examples highlight the vulnerability of elevated tanks to earthquakes and underline the importance of proper design to prevent their collapse.

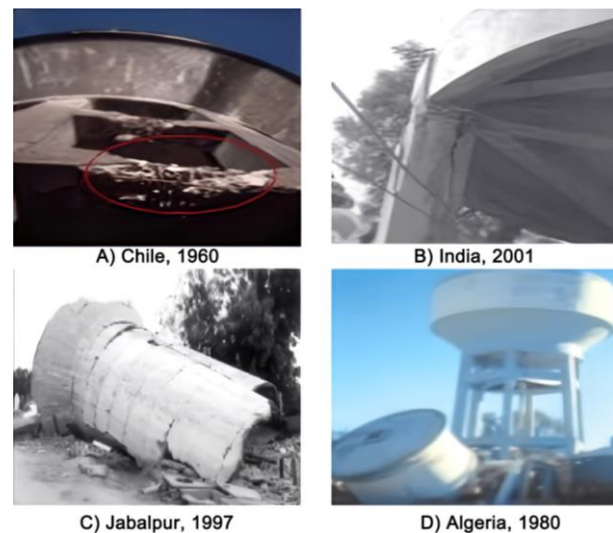


Figure 1. Buildings collapsed in the earthquake

Studies at Ain Shams University, Egypt, on elevated water tanks, essential for water distribution, highlighted seismic safety concerns due to significant stresses during earthquakes. Based on the Egyptian code ECP-201, the research analyzed 108 models using the pushover method, revealing that the response modification factor (R) varies with tank height and seismic zone, requiring adjustments for specific conditions [19], [20].

On the other hand, in India, studies evaluated tank height, ductility, seismic zone, and soil type, referencing international standards such as the Algerian code (R=2) and Eurocode (R=1). These studies proposed a more adaptive standard, emphasizing the importance of adjusting R according to height and seismic conditions to enhance structural safety [21], [22]. Additional research analyzed the influence of ductility on R, showing that fixed values, like R=4 in IITK-GSDMA and IS 1893, are insufficient. With ductility increasing to 8, R values reached up to 9, underscoring the correlation between ductility and R, and the need for flexible seismic design approaches [23], [24].

Finally, the relevance of the response reduction factor (R) in the seismic design of structures, especially in water tanks, was also highlighted in India. The variability of R values in different international codes, such as IBC-2000,

ACI 350.3 and Eurocode 8, was highlighted, pointing out the lack of consensus on these values. In addition, the need for further research on the influence of viscous dampers on the R-factor and the application of methods based on finite element analysis to improve the accuracy in seismic design was raised [25], [26], [27].

This study analysed the structural challenges of elevated tanks, focusing on the effects of height and liquid volume on the seismic reduction factor (R). Using a non-linear static approach using the pushover method, the research incorporated Loreto-specific seismic parameters to propose updates to the Peruvian E.030 standard. Structural designs complied with stiffness guidelines, ensuring drifts between 0.6% and 0.7%. A total of 63 models were evaluated, systematically varying fluid height and volume, applying incremental displacements until structural instability was reached.

2. Materials and Methods

This study followed the Peruvian Standard E.030 Seismic Resistant Design [5], focusing on seismic hazard requirements from Chapter 2. Models of elevated tanks with heights of 12 to 30 meters and liquid volumes from 10 m³ to 30 m³ (in 2.5 m³ intervals) were analyzed, ensuring relative displacements between 6 and 7 per mille to meet stiffness limits. As E.030 does not specify a response reduction factor (R) for pendulum-type structures, ACI 350.3 was used to account for the dynamic properties of liquids, including impulsive and convective masses. Two approaches were explored: one considering dynamic masses and the other treating the liquid as a static element. Representative cases (volumes of 10, 20, and 30 m³ at heights of 12, 21, and 30 meters) identified critical combinations impacting dynamic forces, informing a pushover analysis to estimate an R factor for the 63 tank models. The methodology integrated normative criteria with advanced analysis, ensuring compliance with seismic-resistant design standards while addressing gaps in Peruvian regulations for pendulum-type structures.

2.1. Seismic Analysis

Seismic analysis of buildings is crucial for structural safety, especially in earthquake-prone regions. This study followed the Technical Building Standard E.030 [5], which ensures that structures resist the expected seismic effects. Focused on the Mara ñón-Andoas de Loreto region, a zone of low seismic activity, which is shown in Figure 2, the study used parameters such as seismic zone (Z = 0.25), use factor (U = 1.5) for category A structures and soil factor (S = 1.4) for S3 type soils. The seismic force reduction (R) and base reduction (Ro) coefficients were selected to ensure stability, and the design spectral periods Tp (1 s) and Tl (1.6 s) were verified, all seismic data are

shown in Table 1. This analysis established a solid framework for designing elevated tanks in low seismic zones, complying with regulatory safety standards.

Table 1. Seismic Parameters E.030 standard

Abbreviation	Description	Factor
Z	Zone 2	0.25
U	Use factor category A	1.5
C	Seismic Amplification Factor	2.5
S	Soil factor (s3)	1.4
Tp	Period defining the C-factor platform	1
Tl	Period defining the beginning of the C-factor zone with constant displacement.	1.6
Ro	Basic Reduction Coefficient	5
Ia	Height Irregularity	1
Ip	Irregularity in plant	1
R	Coefficient of reduction of seismic forces	5

$$S_a = \frac{Z \cdot U \cdot C \cdot S}{R} \cdot g \quad (1)$$



Figure 2. Seismic zones of Peru [5]

2.2. Structuring of Elevated Tank

The structuring of the elevated tank adhered to the stiffness requirements of Standard E.030, ensuring lateral drifts below 7 per thousand, with all 63 models in Table 2

meeting this criterion. Strength guidelines from Standard E.060 were also incorporated, including anchorage lengths to ensure ductile behavior during potential failures [28]. As Peruvian standards lack specific parameters for liquid-containing structures, ACI 350.3-20 [9] was applied to account for the liquid's dynamic behavior, represented by impulsive and convective mass, which significantly affects internal forces, particularly in larger tanks. Smaller tanks benefit from the damping effect of the liquid, known

as the tuned liquid buffer effect, mitigating lateral behavior. A representative sample of models was selected to compare the liquid's dynamic effects with a simplified static mass approach, identifying key differences in structural responses and ensuring compliance with stiffness and ductility requirements. This methodological approach resulted in technically robust, optimized models, contributing to accurate and locally adapted design criteria for liquid-containing structures.

Table 2. Properties of the above-ground tanks analysed

Item	Tank height	Volume of liquid	Columns (cm)	Beams (cm)	Slab thickness (m)	Wall thickness (m)	Concrete strength f_c (kg/cm ⁺)	Drift
T1_M1	12	10	50x50	25x45	0.15	0.20	210	0.00623
T1_M2	12	12.5	50x50	25x45	0.15	0.20	210	0.00647
T1_M3	12	15	50x50	25x45	0.15	0.20	210	0.00671
T1_M4	12	17.5	50x50	30x45	0.15	0.20	210	0.00640
T1_M5	12	20	50x50	30x45	0.15	0.20	210	0.00662
T1_M6	12	22.5	50x50	30x45	0.15	0.20	210	0.00683
T1_M7	12	25	55x55	30x45	0.15	0.20	210	0.00629
T1_M8	12	27.5	55x55	30x45	0.15	0.20	210	0.00648
T1_M9	12	30	55x55	30x45	0.15	0.20	210	0.00666
T2_M1	15	10	50x50	30x50	0.15	0.20	210	0.00606
T2_M2	15	12.5	50x50	30x50	0.15	0.20	210	0.00626
T2_M3	15	15	50x50	30x50	0.15	0.20	210	0.00647
T2_M4	15	17.5	55x55	30x50	0.15	0.20	210	0.00618
T2_M5	15	20	55x55	30x50	0.15	0.20	210	0.00636
T2_M6	15	22.5	55x55	30x50	0.15	0.20	210	0.00654
T2_M7	15	25	60x60	30x50	0.15	0.20	210	0.00627
T2_M8	15	27.5	60x60	30x50	0.15	0.20	210	0.00643
T2_M9	15	30	60x60	30x50	0.15	0.20	210	0.00659
T3_M1	18	10	60x60	30x50	0.15	0.20	210	0.00635
T3_M2	18	12.5	60x60	30x50	0.15	0.20	210	0.00652
T3_M3	18	15	60x60	30x50	0.15	0.20	210	0.00669
T3_M4	18	17.5	65x65	30x50	0.15	0.20	210	0.00656
T3_M5	18	20	65x65	30x50	0.15	0.20	210	0.00672
T3_M6	18	22.5	65x65	30x50	0.15	0.20	210	0.00687
T3_M7	18	25	70x70	30x50	0.15	0.20	210	0.00670
T3_M8	18	27.5	70x70	30x50	0.15	0.20	210	0.00684
T3_M9	18	30	70x70	30x50	0.15	0.20	210	0.00699
T4_M1	21	10	55x55	30x55	0.15	0.20	210	0.00658
T4_M2	21	12.5	55x55	30x55	0.15	0.20	210	0.00673
T4_M3	21	15	55x55	30x55	0.15	0.20	210	0.00690
T4_M4	21	17.5	55x55	30x60	0.15	0.20	210	0.00617

Table 2 continued

T4_M5	21	20	55x55	30x60	0.15	0.20	210	0.00632
T4_M6	21	22.5	55x55	30x60	0.15	0.20	210	0.00646
T4_M7	21	25	60x60	30x60	0.15	0.20	210	0.00624
T4_M8	21	27.5	60x60	30x60	0.15	0.20	210	0.00637
T4_M9	21	30	60x60	30x60	0.15	0.20	210	0.00651
T5_M1	24	10	60x60	30x60	0.15	0.20	210	0.00629
T5_M2	24	12.5	60x60	30x60	0.15	0.20	210	0.00643
T5_M3	24	15	60x60	30x60	0.15	0.20	210	0.00657
T5_M4	24	17.5	65x65	30x60	0.15	0.20	210	0.00649
T5_M5	24	20	65x65	30x60	0.15	0.20	210	0.00662
T5_M6	24	22.5	65x65	30x60	0.15	0.20	210	0.00675
T5_M7	24	25	70x70	30x60	0.15	0.20	210	0.00670
T5_M8	24	27.5	70x70	30x60	0.15	0.20	210	0.00682
T5_M9	24	30	70x70	30x60	0.15	0.20	210	0.00694
T6_M1	27	10	65x65	30x65	0.15	0.20	210	0.00621
T6_M2	27	12.5	65x65	30x65	0.15	0.20	210	0.00634
T6_M3	27	15	65x65	30x65	0.15	0.20	210	0.00646
T6_M4	27	17.5	65x65	30x65	0.15	0.20	210	0.00658
T6_M5	27	20	65x65	30x65	0.15	0.20	210	0.00670
T6_M6	27	22.5	65x65	30x65	0.15	0.20	210	0.00683
T6_M7	27	25	70x70	30x65	0.15	0.20	210	0.00672
T6_M8	27	27.5	70x70	30x65	0.15	0.20	210	0.00684
T6_M9	27	30	70x70	30x65	0.15	0.20	210	0.00695
T7_M1	30	10	70x70	30x65	0.15	0.20	210	0.00636
T7_M2	30	12.5	70x70	30x65	0.15	0.20	210	0.00646
T7_M3	30	15	70x70	30x65	0.15	0.20	210	0.00657
T7_M4	30	17.5	75x75	30x70	0.15	0.20	210	0.00652
T7_M5	30	20	75x75	30x70	0.15	0.20	210	0.00661
T7_M6	30	22.5	75x75	30x70	0.15	0.20	210	0.00670
T7_M7	30	25	75x75	30x70	0.15	0.20	210	0.00680
T7_M8	30	27.5	75x75	30x70	0.15	0.20	210	0.00689
T7_M9	30	30	75x75	30x70	0.15	0.20	210	0.00700

Figure 3 illustrates structural models types 1 to 7, differentiated by height, ranging from 12 metres (type 1) to 30 metres (type 7) in uniform increments. For model type 1, nine volume variations were analysed, with capacities from 10 m³ to 30 m³ in 2.5 m³ increments, as detailed in Table 2. Each model's geometry was preliminarily evaluated to ensure compliance with the E.030 standard's stiffness requirements, limiting lateral drift to 7 per thousand. This analysis validated the structural configurations and provided a solid basis for subsequent seismic analyses.

2.3. Dynamic Properties in Liquids

The analysis of the dynamic properties of liquids followed the guidelines of ACI 350.3-20 [9], which accounts for two key components: impulsive mass and convective mass. Since the Peruvian Standard E.030 does not include these dynamic characteristics, a comparative evaluation was conducted. The study analyzed scenarios with and without these components to identify the most conservative and critical behavior for structural design, ensuring a robust approach to address dynamic effects.

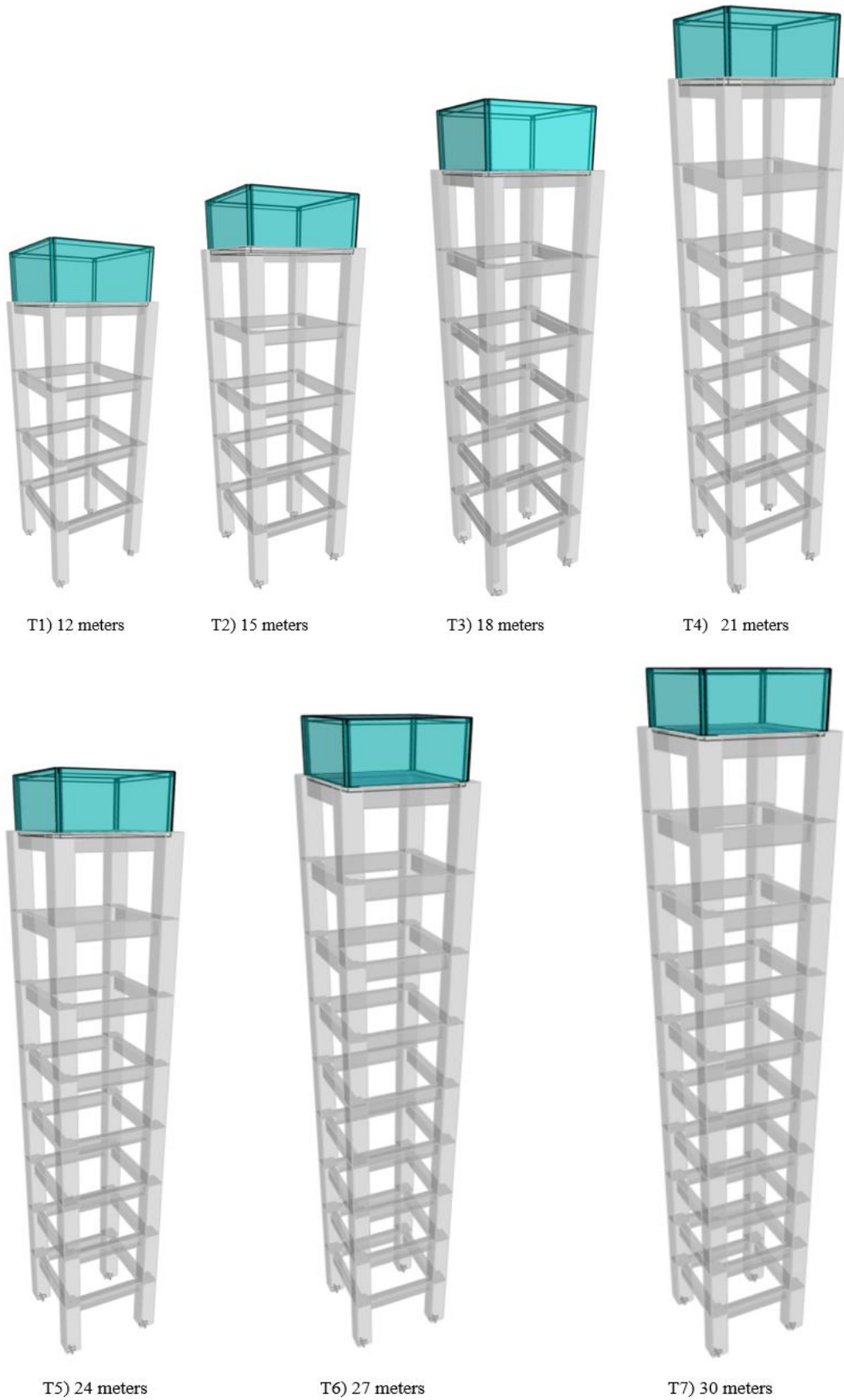


Figure 3. Elevated tank models in ETABS

2.3.1. Preliminary Dynamic Analysis

Equations were developed to calculate the dynamic properties of liquids, including impulsive weight (P_i), convective weight (P_c), and wall weight (P_m), used to determine the total design shear (V_{total}), combining tank dynamics and structural inertial forces. Based on ACI 350.3-20 [9], these equations were applied to type 1, type 4, and type 7 models with liquid volumes of 10, 20, and 30 m³. The most critical cases were then identified to determine configurations producing the highest seismic shears.

2.3.2. Impulsive Weight (P_i)

The impulsive weight is the seismic load from the movement of the liquid inside the tank during an earthquake, caused by the inertia of the liquid moving, impacting the walls and base of the tank. Its magnitude depends on the frequency of the earthquake and the height of the liquid [9], [29].

The impulsive weight was calculated using equation (2), as a function of the height of the liquid, the tank dimensions in plan (4 m × 4 m) and the specific gravity of the liquid (1,000 kg/m³):

$$P_i = \frac{\tanh(0.866 \frac{L_{solera}}{H_{liquid}})}{0.866 \frac{L_{solera}}{H_{liquid}}} \cdot W_{liquid} \quad (2)$$

2.3.3. Convective Weight (P_c)

The convective weight is the load uniformly distributed in the tank due to the general motion of the liquid during an earthquake, and is used to evaluate the total load at the base of the tank [9], [30].

The convective weight, associated with the dynamic wave-like motion, was estimated with equation (3).

$$P_c = 0.264 \cdot \frac{L_{solera}}{H_{liquid}} \cdot \tanh(3.16 \cdot \frac{H_{liquid}}{L_{solera}}) \cdot W_{liquid} \quad (3)$$

2.3.4. Weight of Walls (P_m)

The weight of the tank walls, which resist both static and dynamic loads during an earthquake, is considered when calculating the seismic reaction forces and the energy dissipation capacity of the tank. These forces act on the columns and the base, transmitting loads to the ground [9][31]. The weight of the walls, dependent on the ratio of the tank dimensions to the liquid height, was calculated by equation (4):

$$P_m = Weight_{wall} * (0.015 * (\frac{L}{H_{liquid}})^2 - 0.1908 * (\frac{L}{H_{liquid}}) + 1.021) \quad (4)$$

2.3.5. Total Shear (V_{total})

The total shear is the internal force acting on the foundations of the structure due to dynamic interaction with the ground during a seismic event [9], [32].

The total shear in the structure, including the dynamic forces of the fluid and the weight of the supporting structure, was determined with equation (5):

$$V_{total} = \sqrt{(P_i + P_m + P_s)^2 + P_c^2 + P_{eg}^2} \quad (5)$$

In this equation, P_s corresponds to the weight of the supporting structure, while P_{eg} , related to the lateral thrust, was considered zero due to the configuration of the elevated tanks.

2.3.6. Fluid Analysis

The results showed that the dynamic liquid properties approach, based on ACI 350.3-20 [9], generates lower seismic shear values due to damping effects from convective motion and impulsive mass interaction, but it is less conservative for ensuring maximum safety in elevated tanks under seismic forces. For smaller volumes (10 m³ and 20 m³), the liquid acts as a tuned damper, reducing seismic demands, while for larger volumes (30 m³ or more), the added dynamic weight increases design demands. To ensure robustness, the static model was chosen, providing a higher safety margin by considering greater inertial mass, which increases seismic forces. Critical models were identified based on seismic shear, revealing the most demanding geometry and volume combinations, which informed conservative design recommendations for structural integrity under severe seismic conditions. The static model aligns better with Peruvian regulations, which do not account for dynamic liquid properties, emphasizing the importance of adapting methodologies to local standards. Table 3 summarizes the weights of tank components (water, cylinder, walls, support) and total weight for both dynamic and static models, analyzing variations across three models (T1, T4, T7) and configurations (M1, M5, M9).

2.4. Pushover Curve

The pushover curve, shown in Figure 4, illustrates the relationship between the lateral deformation of the structure (vertical axis) and the associated shear [33]. Generated using ETABS, this graph models the 63 structural designs analyzed in the study, including all frame elements (beams and columns). The analysis employed displacement control, progressively forcing elements into the inelastic range, characterized by a loss of stiffness. To accurately model this behavior, the inertial properties of cracked elements were reduced. The process continued incrementally until reaching a critical displacement level, marked by a drop in the curve, indicating structural collapse due to instability. This approach enabled the evaluation of the non-linear material response and seismic capacity, offering critical insights for designing and assessing structures in seismic zones.

Table 3. Properties of the Elements of the Elevated Tank

Item	Total weight of the Liquid Dynamic Model						Modelo estático			Total (ton)
	Pi (ton)	Pc (ton)	Pm (ton)	Ps (ton)	Peg (ton)	Ptotal (ton)	Pliquid (ton)	Psupport (ton)	Pwalls (ton)	
T1_M1	1.804	7.725	6.105	45.520	0.000	53.985	10.000	45.520	14.592	70.112
T1_M5	7.161	12.778	8.245	48.544	0.000	65.214	20.000	48.544	14.592	83.136
T1_M9	15.451	15.235	9.962	54.333	0.000	81.188	30.000	54.333	14.592	98.925
T4_M1	1.804	7.725	6.105	100.838	0.000	109.021	10.000	100.838	14.592	125.430
T4_M5	7.161	12.778	8.245	104.315	0.000	120.401	20.000	104.315	14.592	138.907
T4_M9	15.451	15.235	9.962	115.302	0.000	141.537	30.000	115.302	14.592	159.894
T7_M1	1.804	7.725	6.105	204.496	0.000	212.546	10.000	204.496	14.592	229.088
T7_M5	7.161	12.778	8.245	229.120	0.000	244.860	20.000	229.120	14.592	263.712
T7_M9	15.451	15.235	9.962	16267.120	0.000	16292.540	30.000	16267.120	14.592	16311.712

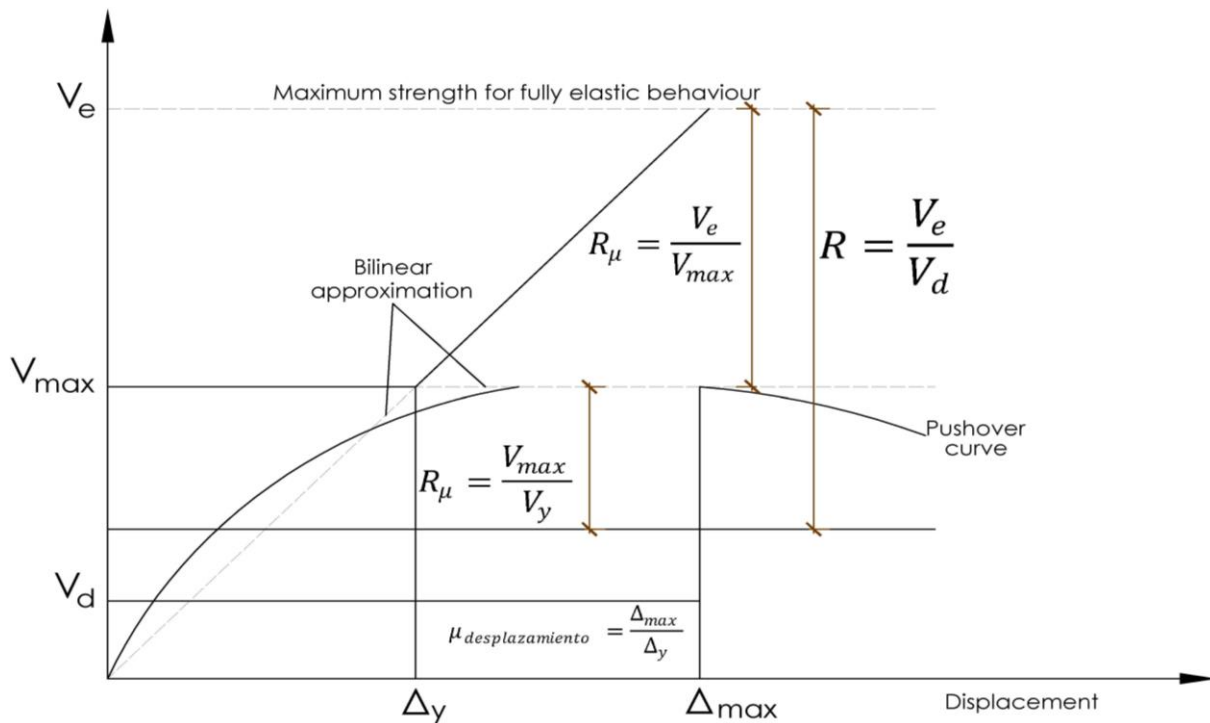


Figure 4. Pushover curve

2.4.1. Seismic Reduction Factor (R)

The seismic reduction factor (R) is calculated using equation 6, which details the ductility factor (Ru), lateral resistance (Rs) and redundancy factor (RR). These factors reflect the capacity of the structure to resist deformations, dissipate energy and resist seismic loads, adjusting the design loads according to its dynamic behaviour.

$$R = R_{\mu} \times R_s \times R_R \tag{6}$$

2.4.2. Strength Reduction Factor for Ductility (Rμ)

The Rμ factor represents the ratio between the maximum load capacity of a structure, corresponding to the collapse point on the Pushover curve, and the initial

load capacity, corresponding to the yield point. This parameter measures the ability of the structure to deform plastically without losing its stability and strength. The Rμ factor is calculated by equation 7, where Δdisplacement, shown in Figure 4, establishes the relationship between the maximum displacement and the yield displacement.

$$R_{\mu} = \frac{\mu_{displacement}^{-1}}{\phi} + 1 \tag{7}$$

On the other hand φ is calculated by equation 8:

$$\phi = 1 + \frac{T_g}{3T} - \frac{3T_g}{4T} \exp \left[-3 \left(\ln \frac{T}{T_g} - 0.25 \right)^2 \right] \tag{8}$$

Where:

T_g: Is the period of the soil, which, due to the characteristics of a soft soil, was considered equal to the period T_L.

T: Is the period of the structure, determined when the elements begin to crack and experience non-linear behaviour.

2.4.3. Over-Resistance Factor (R_s)

The over-resistance factor R_s, measures the capacity of a structure to resist seismic loads greater than its design, comparing its ultimate capacity with the design capacity, which in our case was carried out using the design combinations stipulated in the E060 reinforced concrete standard [34].

$$R_s = \frac{V_{max}}{V_d} \quad (9)$$

2.4.4. Redundancy Factor (R_R)

The redundancy factor measures the capacity of a structure to redistribute seismic loads when one or more of its elements fail, which improves its resistance to partial failure and ensures overall stability [35]. This factor reflects the efficiency of the structure to withstand seismic loads through the presence of redundant elements that reinforce its response capacity, when having a portal frame system this value is reflected in equation 10.

$$R_R = 0.71 \quad (\text{support aperturado, ATC-19}) \quad (10)$$

2.5. Cracked Beams for the Non-Linear Model

For the modelling of the beams, it was necessary to evaluate the parameters that enter the inelastic zone, which means that the element loses stiffness due to the cracked section, which affects its capacity to resist bending and shear forces. In the pushover analysis, to reflect this non-linear behaviour, the inertia of the section was set to 0.3, according to ASCE (American Society of

Civil Engineers) [36]. The assignment of this value was crucial to obtain a more accurate representation of the structural response to dynamic loading, as it allowed the greater flexibility and deformation of the structure compared to a beam without cracking to be adequately modelled.

2.6. Cracked Columns for the Non-Linear Model

Columns, when they enter the inelastic zone, lose stiffness due to cracked sections, which affects their ability to resist compressive and bending forces. In the pushover analysis, to reflect this behaviour, the inertia of the section was set to 0.7, in accordance with ASCE (American Society of Civil Engineers) [36]. The placement of this value was crucial to obtain a more accurate representation of the structural response to dynamic loading, as it allowed the greater flexibility and deformation of the structure compared to a column without cracking to be adequately modelled.

2.7. Table of Steels in the Frame Elements

Table 4 provides detailed properties of elevated tanks ranging from 12 m to 30 m in height, classified into types T1 through T7, each with nine models and liquid volumes from 10 m³ to 30 m³ increasing in 2.5 m³ increments. The steel used in column structures primarily consists of 3/4" rods, with larger tanks occasionally incorporating 5/8" rods for additional strength. For beams, the steel distribution is divided into upper and lower sections, remaining relatively consistent for each height but scaling proportionally with the liquid volume. Higher-capacity models frequently use a combination of 3/4" and 5/8" rods to support the increased liquid weight. This data offers a comprehensive view of how structural properties, including steel specifications and distribution, vary with tank height and volume.

Table 4. Steels placed in the frame elements

Item	Tank height (m)	Liquid volume (m ³)	Steel in Columns	Steel in Beam i-j upper part	Steel in Beam i-j lower part
T1_M1	12	10	8 Ø 3/4"	3 Ø 3/4"	3 Ø 3/4"
T1_M2	12	12.5	8 Ø 3/4"	3 Ø 3/4"	3 Ø 3/4"
T1_M3	12	15	8 Ø 3/4"	3 Ø 3/4"	3 Ø 3/4"
T1_M4	12	17.5	8 Ø 3/4"	3 Ø 3/4"	3 Ø 3/4"
T1_M5	12	20	8 Ø 3/4"	3 Ø 3/4"	3 Ø 3/4"
T1_M6	12	22.5	8 Ø 3/4"	3 Ø 3/4"	3 Ø 3/4"
T1_M7	12	25	12 Ø 3/4"	3 Ø 3/4"	3 Ø 3/4"
T1_M8	12	27.5	12 Ø 3/4"	3 Ø 3/4"	3 Ø 3/4"
T1_M9	12	30	12 Ø 3/4"	2 Ø 3/4" + 2 Ø 5/8"	2 Ø 3/4" + 2 Ø 5/8"
T2_M1	15	10	12 Ø 3/4"	3 Ø 3/4"	3 Ø 3/4"
T2_M2	15	12.5	12 Ø 3/4"	3 Ø 3/4"	3 Ø 3/4"

Table 4 continued

T2_M3	15	15	12 Ø 3/4"	2 Ø 3/4" + 2 Ø 5/8"	2 Ø 3/4" + 2 Ø 5/8"
T2_M4	15	17.5	12 Ø 3/4"	2 Ø 3/4" + 2 Ø 5/8"	2 Ø 3/4" + 2 Ø 5/8"
T2_M5	15	20	12 Ø 3/4"	2 Ø 3/4" + 2 Ø 5/8"	2 Ø 3/4" + 2 Ø 5/8"
T2_M6	15	22.5	12 Ø 3/4"	3 Ø 3/4" + 1 Ø 5/8"	3 Ø 3/4" + 1 Ø 5/8"
T2_M7	15	25	12 Ø 3/4"	3 Ø 3/4" + 1 Ø 5/8"	3 Ø 3/4" + 1 Ø 5/8"
T2_M8	15	27.5	12 Ø 3/4"	3 Ø 3/4" + 1 Ø 5/8"	3 Ø 3/4" + 1 Ø 5/8"
T2_M9	15	30	12 Ø 3/4"	3 Ø 3/4" + 1 Ø 5/8"	3 Ø 3/4" + 1 Ø 5/8"
T3_M1	18	10	16 Ø 3/4"	2 Ø 3/4" + 2 Ø 5/8"	2 Ø 3/4" + 2 Ø 5/8"
T3_M2	18	12.5	16 Ø 3/4"	3 Ø 3/4" + 1 Ø 5/8"	3 Ø 3/4" + 1 Ø 5/8"
T3_M3	18	15	16 Ø 3/4"	3 Ø 3/4" + 1 Ø 5/8"	3 Ø 3/4" + 1 Ø 5/8"
T3_M4	18	17.5	12 Ø 3/4"	4 Ø 3/4"	4 Ø 3/4"
T3_M5	18	20	12 Ø 3/4"	4 Ø 3/4"	4 Ø 3/4"
T3_M6	18	22.5	16 Ø 3/4"	4 Ø 3/4"	4 Ø 3/4"
T3_M7	18	25	16 Ø 3/4"	4 Ø 3/4"	4 Ø 3/4"
T3_M8	18	27.5	16 Ø 3/4"	4 Ø 3/4"	4 Ø 3/4"
T3_M9	18	30	16 Ø 3/4"	4 Ø 3/4"	4 Ø 3/4"
T4_M1	21	10	12 Ø 3/4"	4 Ø 3/4"	4 Ø 3/4"
T4_M2	21	12.5	12 Ø 3/4"	4 Ø 3/4"	4 Ø 3/4"
T4_M3	21	15	12 Ø 3/4"	4 Ø 3/4"	4 Ø 3/4"
T4_M4	21	17.5	12 Ø 3/4"	4 Ø 3/4"	4 Ø 3/4"
T4_M5	21	20	12 Ø 3/4"	4 Ø 3/4"	4 Ø 3/4"
T4_M6	21	22.5	12 Ø 3/4"	4 Ø 3/4"	4 Ø 3/4"
T4_M7	21	25	16 Ø 3/4"	4 Ø 3/4"	4 Ø 3/4"
T4_M8	21	27.5	16 Ø 3/4"	4 Ø 3/4"	4 Ø 3/4"
T4_M9	21	30	16 Ø 3/4"	4 Ø 3/4"	4 Ø 3/4"
T5_M1	24	10	12 Ø 3/4"	4 Ø 3/4"	4 Ø 3/4"
T5_M2	24	12.5	12 Ø 3/4"	4 Ø 3/4"	4 Ø 3/4"
T5_M3	24	15	12 Ø 3/4"	4 Ø 3/4"	4 Ø 3/4"
T5_M4	24	17.5	16 Ø 3/4"	3 Ø 3/4" + 2 Ø 5/8"	3 Ø 3/4" + 2 Ø 5/8"
T5_M5	24	20	16 Ø 3/4"	3 Ø 3/4" + 2 Ø 5/8"	3 Ø 3/4" + 2 Ø 5/8"
T5_M6	24	22.5	16 Ø 3/4"	3 Ø 3/4" + 2 Ø 5/8"	3 Ø 3/4" + 2 Ø 5/8"
T5_M7	24	25	16 Ø 3/4"	4 Ø 3/4" + 1 Ø 5/8"	4 Ø 3/4" + 1 Ø 5/8"
T5_M8	24	27.5	16 Ø 3/4"	4 Ø 3/4" + 1 Ø 5/8"	4 Ø 3/4" + 1 Ø 5/8"
T5_M9	24	30	16 Ø 3/4"	4 Ø 3/4" + 1 Ø 5/8"	4 Ø 3/4" + 1 Ø 5/8"
T6_M1	27	10	16 Ø 3/4"	3 Ø 3/4" + 2 Ø 5/8"	3 Ø 3/4" + 2 Ø 5/8"
T6_M2	27	12.5	16 Ø 3/4"	3 Ø 3/4" + 2 Ø 5/8"	3 Ø 3/4" + 2 Ø 5/8"
T6_M3	27	15	16 Ø 3/4"	3 Ø 3/4" + 2 Ø 5/8"	3 Ø 3/4" + 2 Ø 5/8"
T6_M4	27	17.5	16 Ø 3/4"	3 Ø 3/4" + 2 Ø 5/8"	3 Ø 3/4" + 2 Ø 5/8"
T6_M5	27	20	16 Ø 3/4"	3 Ø 3/4" + 2 Ø 5/8"	3 Ø 3/4" + 2 Ø 5/8"
T6_M6	27	22.5	16 Ø 3/4"	3 Ø 3/4" + 2 Ø 5/8"	3 Ø 3/4" + 2 Ø 5/8"
T6_M7	27	25	20 Ø 3/4"	5 Ø 3/4"	5 Ø 3/4"

Table 4 continued

T6_M8	27	27.5	20 Ø 3/4"	5 Ø 3/4"	5 Ø 3/4"
T6_M9	27	30	20 Ø 3/4"	5 Ø 3/4"	5 Ø 3/4"
T7_M1	30	10	16 Ø 3/4"	5 Ø 3/4"	5 Ø 3/4"
T7_M2	30	12.5	16 Ø 3/4"	5 Ø 3/4"	5 Ø 3/4"
T7_M3	30	15	16 Ø 3/4"	5 Ø 3/4"	5 Ø 3/4"
T7_M4	30	17.5	20 Ø 3/4"	5 Ø 3/4"	5 Ø 3/4"
T7_M5	30	20	20 Ø 3/4"	5 Ø 3/4"	5 Ø 3/4"
T7_M6	30	22.5	20 Ø 3/4"	5 Ø 3/4"	5 Ø 3/4"
T7_M7	30	25	20 Ø 3/4"	4 Ø 3/4" + 2 Ø 5/8"	4 Ø 3/4" + 2 Ø 5/8"
T7_M8	30	27.5	20 Ø 3/4"	4 Ø 3/4" + 2 Ø 5/8"	4 Ø 3/4" + 2 Ø 5/8"
T7_M9	30	30	20 Ø 3/4"	4 Ø 3/4" + 2 Ø 5/8"	4 Ø 3/4" + 2 Ø 5/8"

2.7.1. Graphical Representation of Steel in the Column

Figure 5 shows a cross-section schematic of the detailed steel design for the elevated tank columns, complementing Table 4 of model T_M1. The design includes evenly distributed 3/4" steel rods with 3/8" stirrups, strategically arranged to enhance structural strength and stability. The rods are spaced 10 cm apart, ensuring adequate support for the tank's liquid volume.

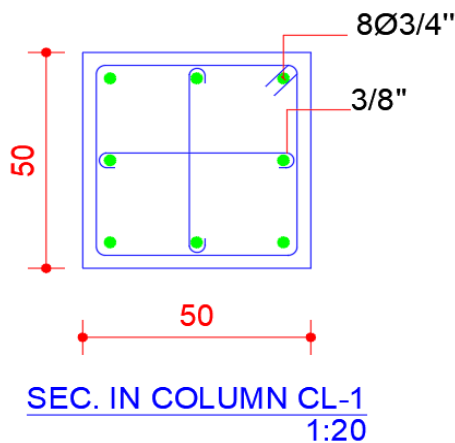


Figure 5. Column cross-section

2.7.2. Graphical Representation of Steel in the Beam

Figure 6 illustrates the steel layout of the beam, as detailed in T1_M1 of Table 4, with 3/4" rods uniformly placed at both the top and bottom. This strategic design ensures adequate reinforcement to efficiently support seismic loads. The arrangement enhances structural resistance to static and dynamic stresses, while the optimized distribution and quantity of steel improve stability and force dissipation during seismic events, ensuring durability and functionality.

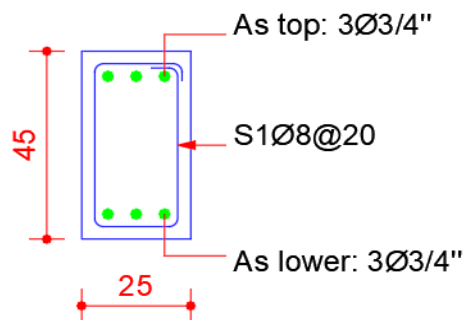


Figure 6. Beam cross-section

2.8. Seismic Records

According to the E.030 seismic-resistant design standard [5], 3 pairs of seismic records must be used for the time-history and compatible spectrum analysis, in order to evaluate how the structures respond to different seismic events. In our research, 3 pairs of seismic records have been selected, which are shown in table 5, corresponding to events that occurred in the department of Loreto, with magnitudes that vary between 4.5 and 5.8, as well as depths ranging between 95 km and 126 km. These records, obtained from specific seismic stations, provide a solid basis for analysing the structural response, allowing a comparative study that is crucial for the design and evaluation of the seismic safety of structures [37].

2.9. Baseline Correction of Seismic Records

Baseline correction is a crucial step in seismic analysis, removing unwanted deviations from data to provide a more accurate representation of events [38]. Figure 7 shows the seismic event in Loreto on 20 August 2023, with the blue curve representing the corrected record processed using SeismoSignal software and the lead line showing the original, untreated record from CISMID. The graph, depicting acceleration over the event's duration, highlights

how the correction eliminates perturbations and deviations, offering a precise view of seismic forces, while the lead line reveals uncorrected fluctuations and distortions in the raw data. This process ensures reliable data and facilitates detailed analysis of Loreto's seismic response, critical for assessing structural impacts.

conditions of the elevated tank, allowing to more accurately simulate how the elevated tank structure would respond to the recorded seismic events. This ensures that the analysis reflects the possible dynamic responses of the elevated tank under seismic loads, ensuring its structural behaviour under extreme conditions.

2.10. Seismic Record Scaling Using SeismoMatch

Seismic log scaling is a process that adjusts the seismic data obtained to the specific design conditions of a structure [38]. Figure 8 shows the seismic records scaled to the design spectrum for the elevated tank using SeismoMatch, which will be used in the non-linear time-history analysis of the structure. This scaling process is crucial to adjust the seismic records to the specific design

2.11. Non-Linear Analysis by Direct Integration

The nonlinear analysis by direct integration simulates its seismic response considering the structural nonlinearity and the interaction with the fluid. This method evaluates how seismic forces affect both the structure and the fluid, taking into account the plasticity of the materials and the sloshing of the fluid, to predict its behaviour during an earthquake [39].

Table 5. Seismic records

Seismic event	Year	Magnitude (Mw)	Station	Depth (Km)
Loreto, Peru	20/08/2023	4.5	UNAAA (National Autonomous University of Alto Amazonas)	98
Loreto, Peru	17/06/2024	5.8	UNAAA (National Autonomous University of Alto Amazonas)	126
Loreto, Peru	03/05/2024	5.2	UNAAA (National Autonomous University of Alto Amazonas)	95

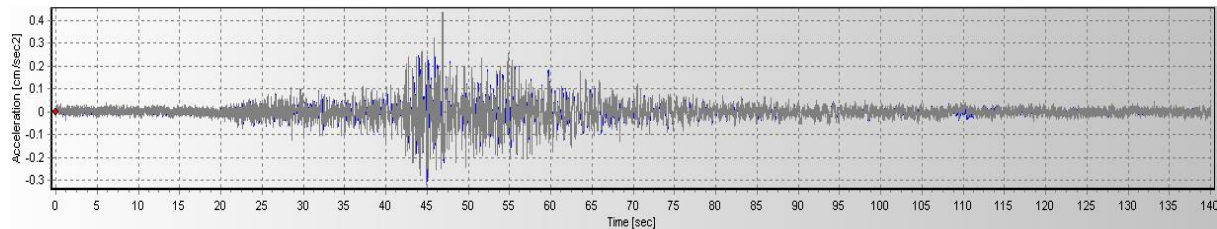


Figure 7. Baseline correction SeismoSignal

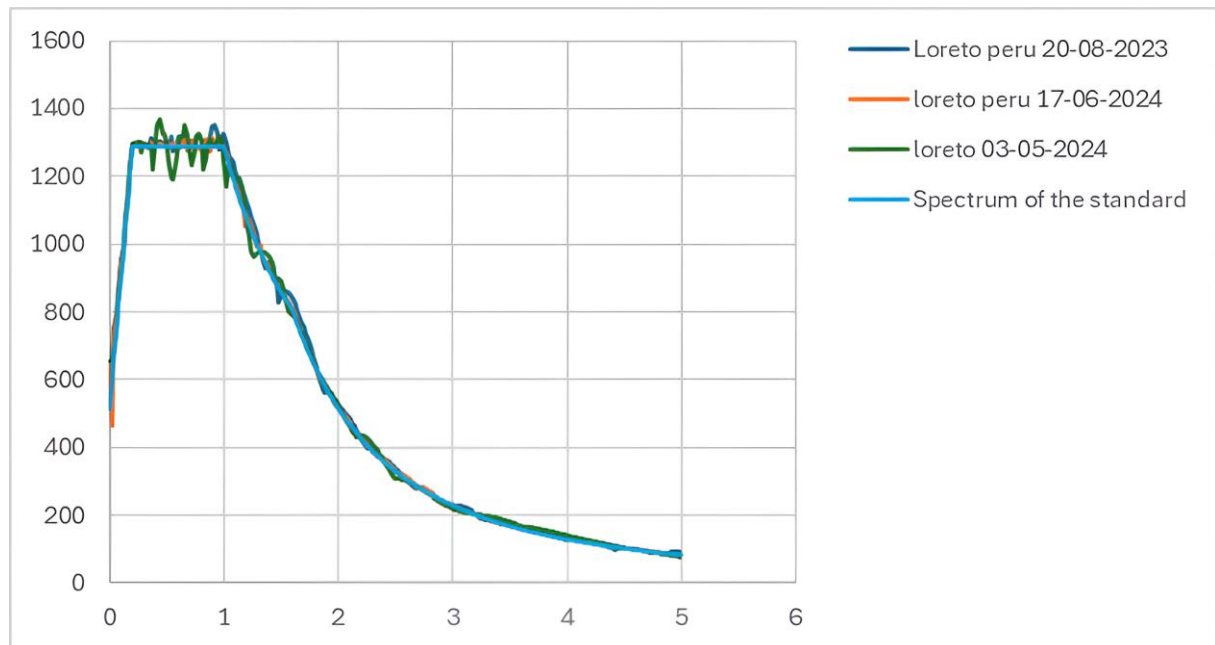


Figure 8. Earthquakes scaled with SeismoMatch

2.12. Assignment of Ball-Point Pens

Plastic hinges are zones where inelastic deformations develop under extreme loads, such as seismic loads [40]. They allow the non-linear behaviour of structures to be modelled more accurately, representing the transition between elastic and inelastic behaviour, and assessing the energy dissipation capacity before collapse. In this research, the designation of plastic hinges was applied in the model of columns and beams of elevated tanks, according to ASCE 41-17, to analyse their seismic response [41], [42]. In this context, Figure 9 shows the phases of structural behaviour, from elastic behaviour to loss of capacity. This approach was preferred over a fibre-based model, as the plastic hinges provide a more accurate representation of inelastic deformations and energy dissipation, ensuring that the elevated tanks can withstand extreme deformations and dissipate seismic energy without collapse.

2.13. Isotropic Hysteresis Model

The isotropic hysteresis model simulates the non-linear behavior of materials under cyclic loading, capturing energy dissipation without altering the material's basic strength or requiring progressive hardening [43]. In this research, it was applied to analyze seismic responses, ensuring energy dissipation and maintaining the integrity of critical elements, such as elevated tanks, under extreme seismic conditions. Aligned with ASCE 41-17 guidelines for non-linear analysis, this model was implemented in ETABS [43], optimizing seismic analysis by offering a streamlined yet effective approach to represent inelastic behavior while preserving structural stability and resilience.

2.14. Plastic Ball Joints on the Beams

The plastic hinges in the beams represent zones of

inelastic rotation, allowing energy dissipation under extreme loads like earthquakes [44]. Figure 10 shows the configuration of plastic hinges in the ETABS model of the elevated tanks, based on ASCE 41-17, table 10-7, item I (A) [45]. For the degree of freedom (B), M3 was chosen for principal bending moments. Transverse reinforcement (C) met confinement requirements, while strain-controlled load capacity (D) extrapolated beyond point 'E' to model non-linear behaviour. Shear stress (E) considered specific load cases, and reinforcement ratio (F) used the "From current design" option to ensure compliance and optimal performance.

2.15. Plastic Signs on Columns

Plastic spherical plain bearings in columns are nonlinear modeling elements used to simulate column behavior under high load or seismic conditions [46], [47]. Figure 11 presents the configuration of plastic hinges in the ETABS model of elevated tanks, following ASCE 41-17, tables 10-8 and 10-9 (A) [47]. The degree of freedom (B) was set to P-M2-M3 to account for axial forces and moments. Concrete behavior (C) was defined as unaffected by inadequate splicing due to compliance with standards. The transverse reinforcement ratio (D) used the "From Current Design" option, ensuring resistance to shear forces. For strain-controlled load capacity (E), extrapolation beyond point "E" was applied to consider residual capacity. Axial load values P (F) were based on gravity and seismic load combinations under critical conditions. Shear demand in bending yield (G) was calculated by the program, reflecting structural analysis results. Finally, the transverse reinforcement spacing ratio (H) also used the "From Current Design" option, meeting regulatory spacing requirements. These configurations accurately modeled the nonlinear column behavior, ensuring performance under the project's load conditions.

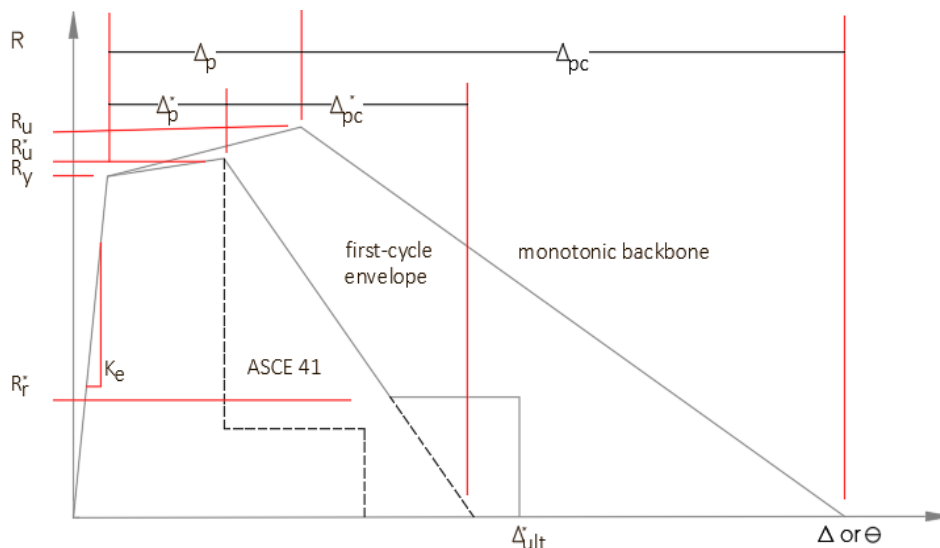


Figure 9. ASCE 41-17

Figure 10. Configuration of Plastic Spherical Plain Bearings on Beams

Figure 11. Configuration of Plastic Spherical Plain Bearings in Columns

3. Results

This section will present the results obtained from the models, whose heights range from 12 to 30 meters, with different volumes assigned to each one. The volumes

considered are: 10 m³, 12.5 m³, 15 m³, 17.5 m³, 20 m³, 22.5 m³, 25 m³, 27.5 m³ and 30 m³. The objective of this analysis is to evaluate how the behavior of each model varies as a function of height and volume, specifically in relation to the seismic reduction factor (R). A detailed view of the

results will be presented, allowing to observe the influences of these parameters on the behavior of the models.

3.1. Models

The analysis of elevated tank models using ETABS software highlights the importance of the key seismic resistance factors: the ductility reduction factor (R_u), the over-resistance factor (R_s) and the redundancy factor (R_r), all determined using formulas 7, 8, 9 and 10, and calculated from pushover curves. These factors are essential for assessing the capacity of a structure to resist and dissipate seismic energy, as well as for calculating the total seismic reduction factor (R_{final}), which adjusts the design seismic loads according to the actual capacity of the structure. For a 12-metre tank, the R_{final} obtained is 7.99, and for a 15-metre tank, it is 8.12, both values very close to the ideal of 8, which evidences a highly ductile behaviour and an adequate capacity to dissipate seismic energy. In the case

of an 18-metre tank, the final R_{final} is 8.03, demonstrating sufficient seismic resistance according to the E-030 standard for portalised systems. A 21-metre tank has an average R_{final} of 3.60, with later models showing improved performance due to higher displacement and deformation capacities. For a 24-metre tank, R_{final} values range from 5.23 to 6.98, indicating that larger liquid volumes increase the capacity to reduce seismic demands. The 27-metre tank achieves R values between 5.60 and 7.90, reflecting moderate stiffness and dissipation capacity, with potential for optimisation to achieve higher ductility. Finally, in a 30-metre tank, the R -values decrease significantly (5.20 to 1.87), reflecting limited plastic behaviour and lower energy dissipation capacity. These results are shown in Table 6 and highlight how height, stiffness and design influence seismic performance, underlining the need to adapt designs to optimise structural resilience and energy dissipation capacity at different tank heights.

Table 6. Results of pushover curve models T1

Item	Vdesign (ton)	Vultima (ton)	Dfluency (cm)	Dmaximo (cm)	Uscrolling	Tg	Tcracked (s)	φ	R_s	R_r	R_u	Rend
T1_M1	18.08	75.71	7.94	29.02	3.65	1.6	0.68	1.75	4.19	0.71	2.52	7.50
T1_M2	18.73	75.45	7.82	28.83	3.69	1.6	0.69	1.72	4.03	0.71	2.56	7.32
T1_M3	19.37	75.27	7.82	28.89	3.69	1.6	0.71	1.70	3.89	0.71	2.58	7.13
T1_M4	20.66	77.43	6.73	28.45	4.23	1.6	0.70	1.72	3.75	0.71	2.88	7.66
T1_M5	21.31	77.20	6.71	28.48	4.24	1.6	0.71	1.70	3.62	0.71	2.91	7.49
T1_M6	21.95	78.56	5.69	22.74	4.00	1.6	0.67	1.76	3.58	0.71	2.70	6.87
T1_M7	23.58	97.58	6.27	28.20	4.50	1.6	0.68	1.75	4.14	0.71	3.00	8.83
T1_M8	24.22	97.38	6.25	28.13	4.50	1.6	0.68	1.74	4.02	0.71	3.02	8.61
T1_M9	24.87	101.16	7.18	28.88	4.02	1.6	0.70	1.71	4.07	0.71	2.77	7.99
T2_M1	21.96	83.59	8.55	33.54	3.92	1.6	0.77	1.61	3.81	0.71	2.82	7.62
T2_M2	22.59	83.42	7.32	33.71	4.61	1.6	0.78	1.59	3.69	0.71	3.27	8.58
T2_M3	23.23	87.43	8.44	34.31	4.07	1.6	0.80	1.57	3.76	0.71	2.96	7.90
T2_M4	25.12	98.67	8.07	33.73	4.18	1.6	0.77	1.61	3.93	0.71	2.97	8.30
T2_M5	25.75	98.51	8.06	33.95	4.21	1.6	0.78	1.59	3.83	0.71	3.02	8.20
T2_M6	26.39	101.45	8.78	34.52	3.93	1.6	0.79	1.57	3.84	0.71	2.86	7.82
T2_M7	28.4	114.52	8.14	33.77	4.15	1.6	0.76	1.62	4.03	0.71	2.94	8.42
T2_M8	29.03	114.32	8.004	33.82	4.23	1.6	0.77	1.60	3.94	0.71	3.01	8.42
T2_M9	29.67	113.93	8.17	33.86	4.14	1.6	0.78	1.59	3.84	0.71	2.98	8.12
T3_M1	27.21	108.84	11.74	39.20	3.34	1.6	0.84	1.51	4.00	0.71	2.55	7.24
T3_M2	27.94	111.83	9.70	39.72	4.09	1.6	0.85	1.49	4.00	0.71	3.08	8.75
T3_M3	28.45	108.34	9.83	40.09	4.08	1.6	0.86	1.47	3.81	0.71	3.09	8.36
T3_M4	30.91	122.42	10.24	39.68	3.88	1.6	0.84	1.51	3.96	0.71	2.91	8.18
T3_M5	31.53	97.64	4.19	25.52	6.09	1.6	0.57	1.92	3.10	0.71	3.65	8.03
T3_M6	32.15	127.66	10.21	40.66	3.98	1.6	0.86	1.47	3.97	0.71	3.03	8.53

Table 6 continued

T3_M7	34.75	142.44	10.19	38.77	3.80	1.6	0.84	1.51	4.10	0.71	2.85	8.31
T3_M8	35.37	141.71	10.08	38.42	3.81	1.6	0.85	1.50	4.01	0.71	2.88	8.19
T3_M9	35.99	143.85	10.14	39.51	3.90	1.6	0.86	1.48	4.00	0.71	2.95	8.38
T4_M1	29.07	78.85	9.15	15.84	1.73	1.6	0.94	1.36	2.71	0.71	1.54	2.96
T4_M2	29.68	80.15	9.17	16.92	1.85	1.6	0.96	1.34	2.70	0.71	1.63	3.13
T4_M3	30.29	78.88	9.32	16.25	1.74	1.6	0.97	1.32	2.60	0.71	1.56	2.89
T4_M4	31.58	89.65	8.44	17.70	2.10	1.6	0.91	1.41	2.84	0.71	1.78	3.59
T4_M5	32.2	87.34	8.22	16.42	2.00	1.6	0.92	1.39	2.71	0.71	1.72	3.31
T4_M6	32.82	87.26	8.25	16.55	2.01	1.6	0.93	1.37	2.66	0.71	1.73	3.27
T4_M7	35.42	105.64	7.83	20.17	2.58	1.6	0.92	1.40	2.98	0.71	2.13	4.50
T4_M8	36.04	105.16	7.84	20.07	2.56	1.6	0.93	1.38	2.92	0.71	2.13	4.41
T4_M9	36.66	105.33	7.91	20.28	2.56	1.6	0.94	1.37	2.87	0.71	2.14	4.37
T5_M1	34.39	92.79	8.12	35.09	4.32	1.6	0.96	1.34	2.70	0.71	3.48	6.67
T5_M2	35.00	86.08	8.13	29.66	3.65	1.6	0.97	1.32	2.46	0.71	3.01	5.25
T5_M3	35.61	85.26	8.02	29.63	3.70	1.6	0.99	1.30	2.39	0.71	3.08	5.23
T5_M4	38.74	109.57	8.51	35.96	4.23	1.6	0.98	1.31	2.83	0.71	3.45	6.94
T5_M5	39.35	109.26	8.48	36.44	4.30	1.6	0.99	1.30	2.78	0.71	3.54	6.98
T5_M6	39.97	108.72	8.48	36.02	4.25	1.6	1.00	1.28	2.72	0.71	3.53	6.83
T5_M7	43.29	121.52	8.66	35.95	4.15	1.6	0.99	1.30	2.81	0.71	3.43	6.84
T5_M8	43.91	120.99	8.87	35.98	4.06	1.6	1.00	1.28	2.76	0.71	3.38	6.62
T5_M9	44.52	120.63	8.88	35.97	4.05	1.6	1.01	1.27	2.71	0.71	3.41	6.56
T6_M1	40.97	114.10	7.95	35.74	4.50	1.6	1.02	1.26	2.78	0.71	3.78	7.48
T6_M2	41.55	110.94	7.85	33.68	4.29	1.6	1.03	1.24	2.67	0.71	3.66	6.93
T6_M3	42.14	140.79	7.74	30.54	3.95	1.6	1.01	1.26	3.34	0.71	3.33	7.90
T6_M4	42.73	140.46	7.68	30.25	3.94	1.6	1.02	1.25	3.29	0.71	3.36	7.83
T6_M5	43.31	140.52	7.69	30.45	3.96	1.6	1.04	1.23	3.24	0.71	3.42	7.87
T6_M6	43.90	140.06	11.03	30.74	2.79	1.6	1.05	1.21	3.19	0.71	2.47	5.60
T6_M7	47.59	178.51	12.05	37.46	3.11	1.6	1.04	1.23	3.75	0.71	2.72	7.25
T6_M8	48.18	177.86	12.30	36.91	3.00	1.6	1.05	1.21	3.69	0.71	2.65	6.94
T6_M9	48.77	177.05	12.22	37.39	3.06	1.6	1.06	1.20	3.63	0.71	2.72	7.01
T7_M1	48.62	112.08	7.57	25.04	3.31	1.6	1.17	1.06	2.31	0.71	3.18	5.20
T7_M2	49.18	90.50	7.43	12.77	1.72	1.6	1.04	1.23	1.84	0.71	1.58	2.07
T7_M3	49.75	109.71	7.49	19.66	2.62	1.6	1.19	1.04	2.21	0.71	2.57	4.02
T7_M4	54.04	92.74	3.47	5.93	1.71	1.6	1.04	1.22	1.72	0.71	1.58	1.92
T7_M5	54.62	92.37	3.48	5.87	1.69	1.6	1.05	1.21	1.69	0.71	1.57	1.88
T7_M6	55.19	91.99	3.49	5.90	1.69	1.6	1.06	1.20	1.67	0.71	1.58	1.87
T7_M7	55.76	91.75	3.49	5.85	1.68	1.6	1.07	1.19	1.65	0.71	1.57	1.83
T7_M8	56.34	91.48	3.49	5.84	1.67	1.6	1.08	1.17	1.62	0.71	1.57	1.81
T7_M9	56.92	91.40	3.49	5.84	1.67	1.6	1.09	1.16	1.61	0.71	1.58	1.80

The analysis of elevated tanks with the ETABS software shows a clear relationship between the liquid volume and the total seismic reduction factor (R_{final}), as shown in Figure 12. For the 12-metre model, R_{final} varies between 6.87 and 8.83, with an average of 7.71, while the 15-metre model ranges between 7.62 and 8.58, with an average of 8.15, both close to the value of 8 used in the design according to the E-030 standard for portal type systems. The 18-metre tank presents values between 7.24 and 8.75, with an average of 8.22, showing a greater energy dissipation capacity as the volume increases. However, in the 21-metre model, R_{final} drops to a range of 2.86 to 4.50 (average 3.60) because the steel does not reach its yield point, limiting ductility. For the 24-metre tank, R_{final} improves significantly (5.23 to 6.98, average 6.43), thanks to a change in the distribution of seismic forces. The 27-metre model shows a range of 5.60 to 7.90 (average 7.20), with a moderate energy dissipation capacity. Finally, the 30-metre tank shows values between 1.87 and 5.20, with an average of 2.49, indicating a stiffer, but less ductile behaviour, although still within a safe range for typical seismic loads. These results highlight how height and structural design influence the seismic resistance and dissipation capacity of elevated tanks.

According to Nasr [19], a comprehensive evaluation of the seismic reduction factor (R) using the Pushover methodology analyzed 108 elevated tanks of varying heights, revealing that as tank height increases, the R -factor decreases significantly. This factor is influenced not only by height but also by the seismic zone and the water mass in the tank, emphasizing the complexity of

these parameters in structural design. Figure 13 corroborates these findings with a scatter plot of 63 models (T1 to T7) showing the relationship between height and the R -factor. The green regression line, representing the maximum behavior, follows the equation $y = -0.064x + 9.598$, with deviations in the T4 model for volumes of 10–22.5 m^3 due to lower ductility and higher stiffness. For larger volumes (25–30 m^3), the steel exhibited more plastic behavior under increasing seismic loads. The red regression line, representing minimal behavior, follows $y = -0.2811x + 10.243$, while the blue intermediate line corresponds to $y = -0.2303x + 11.096$. These equations confirm that taller tanks have lower R -factors, likely due to their greater stiffness and heightened sensitivity to horizontal seismic motions at higher altitudes.

Figure 14 shows a scatter plot illustrating the relationship between height and ultimate shear for 63 models, spanning T1 to T7. The graph shows a trend line. The regression line equation $y = 1.2762x + 80.08$, where the minimum value of the ultimate shear was 75.27 corresponding to T1_M3 with a volume of 15 m^3 and the maximum value was 178.51 corresponding to T6_M7 with a volume of 25 m^3 , as the height of the elevated tanks increases, the ultimate shear increases in absolute terms due to the higher seismic load distribution along the structure. Taller structures, having more mass at the top, generate a higher shear stress at the base, which may compromise the stability of the structure if not properly taken into account.

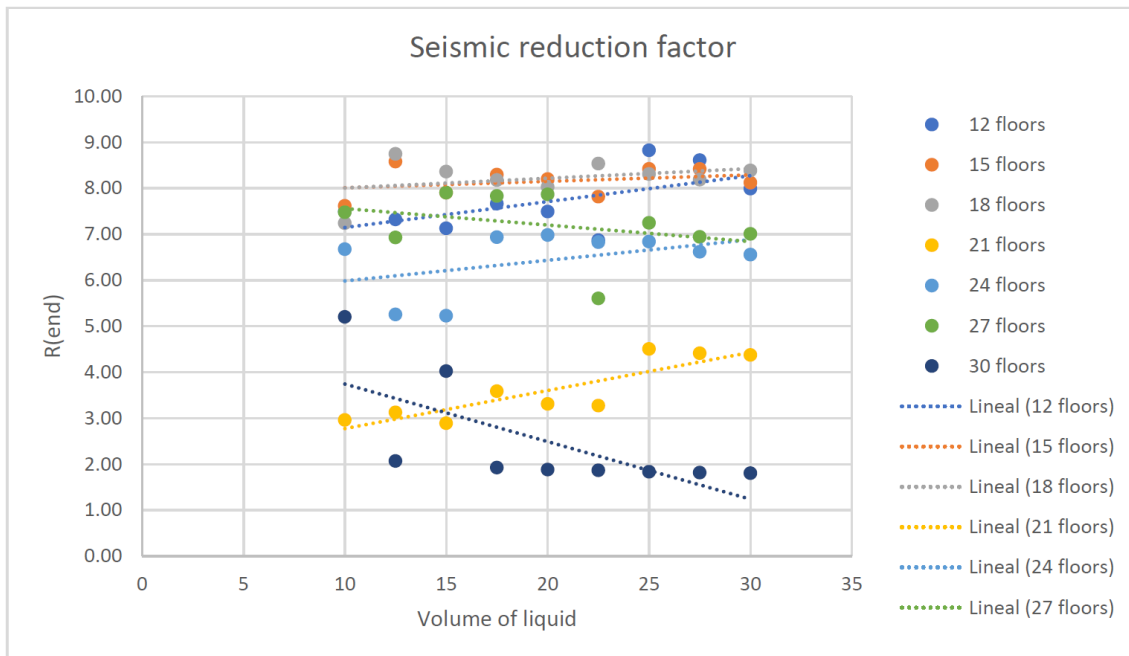


Figure 12. Models

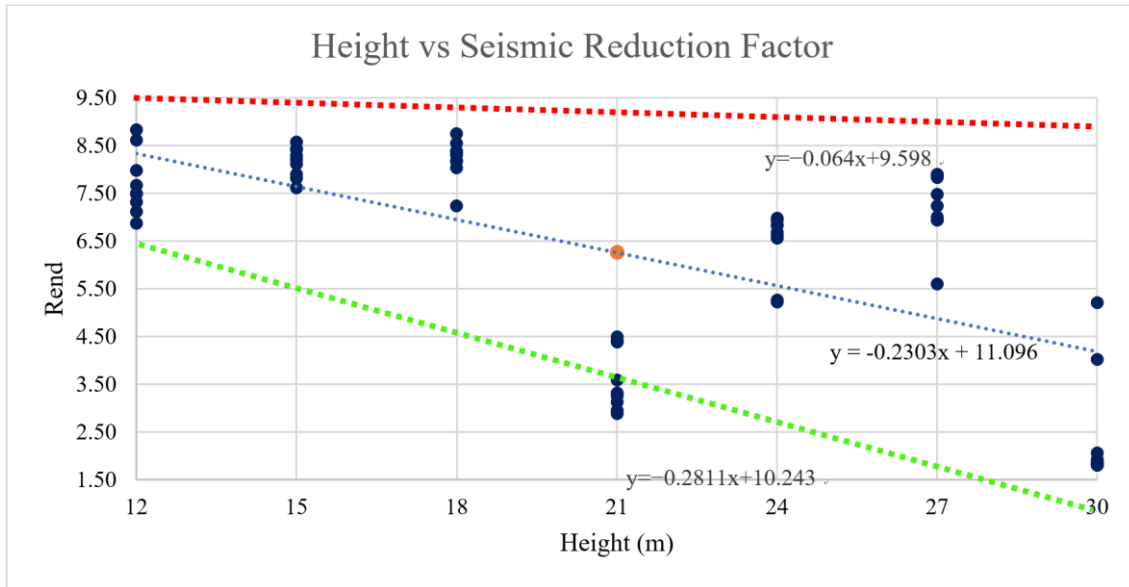


Figure 13. Height of the analyzed models vs Rfinal

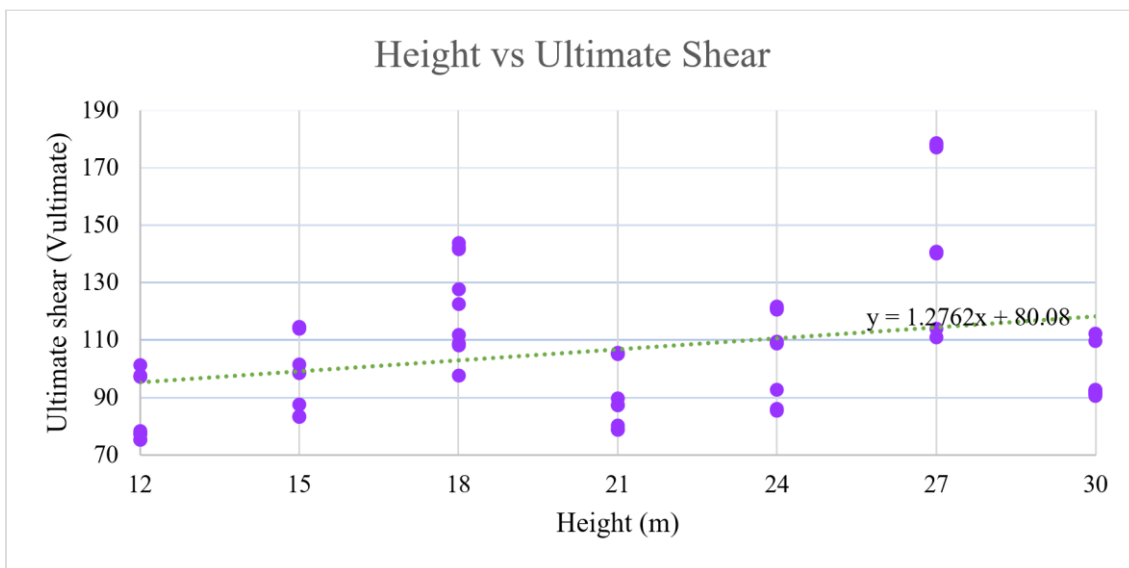


Figure 14. Height of the analyzed models vs. ultimate shear

Figure 15 shows a scatter plot illustrating the relationship between height and maximum displacement for 63 models, spanning T1 to T7. The plot shows a trend line. The regression line equation $y = -0.6769x + 42.233$, where the minimum value of the maximum displacement was 5.84 corresponding to T7_M8 with a volume of 27.5 m^3 and the maximum value was 40.66 corresponding to T3_M6 with a volume of 22.5 m^3 . The 12 - 18m elevated tanks, being more rigid, experience smaller displacements compared to the higher ones. In this range, the maximum displacement is generally smaller due to higher stiffness and structural flexibility. On the other hand, the higher tanks of 21-30m, the maximum displacement increases due to the greater flexibility of the structure, which causes the structure to deform more easily under seismic forces.

Figure 16 shows a scatter plot illustrating the relationship between height and creep displacement (D_{fluence}) for 63 models, spanning T1 to T7. The plot shows a trend line. The regression line equation $y = -0.0546x + 9.153$, where the minimum value of creep displacement was 3.47 corresponding to T7_M4 with a volume of 17.5 m^3 and the maximum value was 12.30 corresponding to T6_M8 with a volume of 27.5 m^3 , as the height of an elevated tank increases, the flexibility of the structure also increases. This implies that taller structures have more capacity to deform under seismic loads, which can generate a larger creep displacement compared to lower structures. This analysis underscores the importance of considering creep displacement when designing elevated tanks, especially for tall structures.

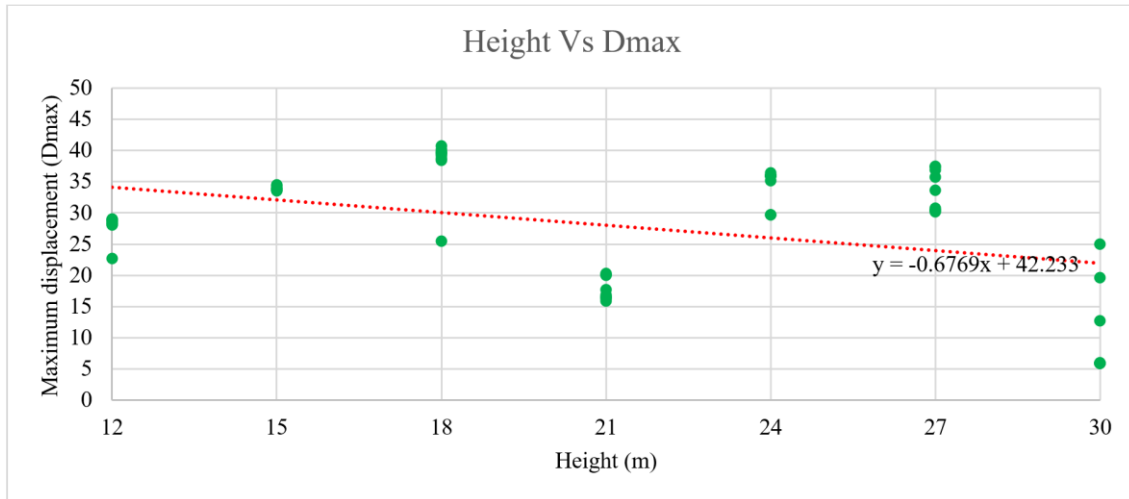


Figure 15. Height of the analyzed models vs. maximum displacement

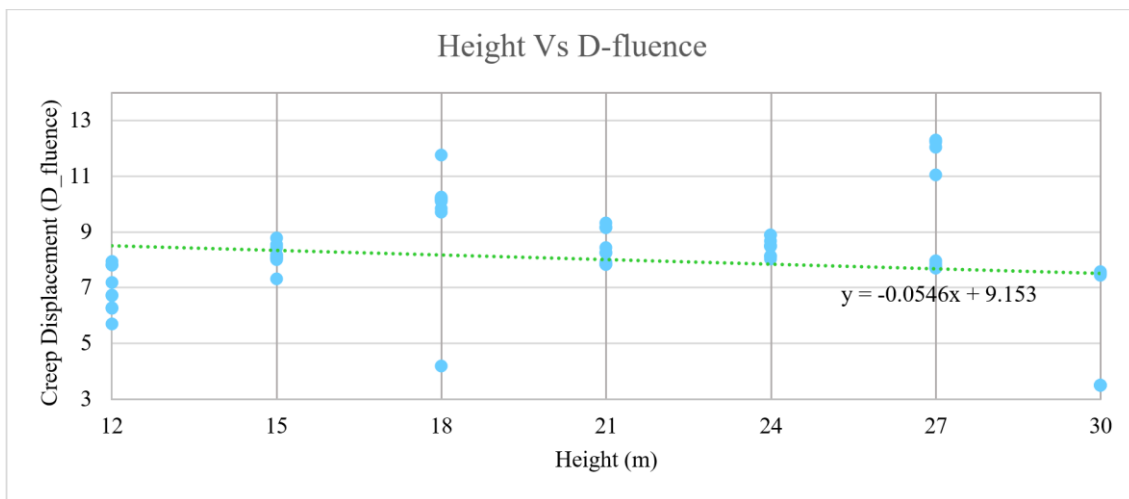


Figure 16. Height of analyzed models vs. creep displacement

3.2. Assumptions and Limitations

The study assumes that structural analysis models accurately represent the behavior of elevated tanks under seismic conditions, although uncertainties exist due to computational modeling and variability in geotechnical and seismic parameters. Key assumptions include that the seismic records used adequately represent the seismic demand in the study region and that the numerical models implemented in ETABS reflect the actual behavior of the structures. However, limitations include the lack of direct experimental validation of the obtained results, dependence on international regulations due to the absence of specific parameters in Peruvian regulations, and the possible variability in materials and construction methods used in the field, which may differ from ideal modeling conditions.

Additionally, soil factors represent a significant source of uncertainty, as geotechnical properties can vary widely within the same region. Normative values from Standard E.030 have been used for soil categorization, but in

practice, specific conditions such as liquefiable soils, expansive clays, or highly variable compaction terrains may affect the seismic response of elevated tanks.

Another relevant limitation is the diversity of tank types used in different regions of the country. This study has focused on elevated tanks with frame-type support, but in other areas, tanks with slender column supports or cantilevered structures may be used, which could respond differently to seismic events. Likewise, fluid-structure interaction in tanks made of different materials, such as steel or reinforced polymers, has not been extensively addressed, which could influence the accuracy of results for systems not considered in this study.

3.3. Broader Applicability

The study findings can be adapted to other regions with different seismic and geotechnical conditions by adjusting seismic reduction coefficients (R) and soil amplification factors (S). Their application in high-seismicity regions

along the Peruvian coast is recommended through complementary studies that consider local subsurface characteristics, such as the presence of liquefiable or highly deformable soils, which could modify the structural response of elevated tanks. Furthermore, the methodology used in this study can serve as a basis for evaluating similar structures in other countries with comparable seismic regulations, provided that appropriate adjustments are made based on local conditions. A fundamental aspect of improving the study's applicability is the calibration of the structural model through back-analysis with data from existing structures in different geographic areas, which would help reduce uncertainty associated with the parameters used in numerical analysis.

3.4. Implementation Plan

The incorporation of the proposed equation into the Peruvian Standard E.030 requires a progressive approach based on a series of technical and administrative steps. First, it is suggested to validate the equation through additional simulations that consider different structural configurations and seismic scenarios, assessing its accuracy by comparison with methodologies established in international regulations. Second, experimental tests on full-scale or reduced-scale physical models of elevated tanks are recommended to verify the correspondence between theoretical values and observed data. A third step involves conducting comparative studies with regulations such as ACI 350.3 and ASCE 41-17, identifying similarities and divergences in design criteria to determine compatibility with the Peruvian regulatory framework. Subsequently, it is suggested to implement pilot studies in existing infrastructure to evaluate the equation's performance under real conditions and analyze its impact on structural safety and construction costs. Finally, for official adoption, the proposal must be reviewed by national regulatory bodies, with the possibility of making adjustments based on the results obtained in the validation and testing phase.

4. Discussions

According to the research C. Mulchandani and J. Amin [48] evaluated the seismic response reduction factor in tanks with capacities from 250 m³ to 2500 m³ and heights between 16 m and 24 m, located in the seismic zone type V of India. Using non-linear static (pushover) analysis, they obtained reduction factors of 5.11 and 9.11, exceeding the range of 2.5 to 4 stipulated by IS 1893. In our study, focusing on 15 m and 24 m tanks, the reduction factors ranged from 2.89 to 8.75, which differs from the values reported by Mulchandani and Amin. This discrepancy is attributed to differences in liquid volume and structural flexibility. However, both studies agree that

larger liquid volume tends to increase the reduction factor, which is consistent with previous observations. In our case, the smaller and stiffer tanks showed lower values (2.89), while the taller and more flexible tanks reached higher values (8.75), in line with the principles of structural dynamics.

According to K. N. Patel and J. A. Amin [49] they analysed reduction factors in elevated tanks with hexagonal and octagonal shapes on medium soils, with volumes from 140 m³ to 2200 m³ and heights of up to 18 m. Using pushover analysis, they reported values between 3.17 and 8.92, exceeding the IITK-GSDM standard of IS 1893, which states 2.5. We agree with Patel and Amin, since, although their tanks have different geometries (hexagonal and octagonal versus the rectangular tanks in our research), the results are similar. In our study, the 15 m rectangular tanks showed a reduction factor of 8.15, and the 18 m rectangular tanks showed a reduction factor of 8.22. This confirms that the increase in height and height of the rectangular tanks is not a factor of 8.15. This confirms that increasing height and volume increases flexibility and energy dissipation capacity, highlighting the importance of geometry and stiffness in seismic behaviour.

According to ACI 350.2 [9], the reduction coefficients are 2.25 for impulsive and 1 for convective seismic action, applicable to anchored tanks with flexible base, although with limitations in the specific application conditions. In our study, by pushover analysis, a reduction coefficient of 2.49 was determined for 30 m tanks in seismic zone 2, which is reasonably in line with the standard. However, we disagree in cases of lower tanks, as we observed higher values, such as 7.20 for a 27 m tank. The 12, 15 and 18 m models showed coefficients between 7 and 8, indicating greater flexibility and energy dissipation. For a 24 m tank, the coefficient was 3.60, exceeding the values proposed by ACI 350.2.

The E.030 standard does not specify reduction factors for inverted pendulums, with the value of 8 for portal frames commonly used as a reference. Our study supports this practice, with an average factor of 8.15 for 15 m tanks and 8.22 for 18 m tanks, aligning with the reference value. These findings highlight the need for clearer guidelines, while confirming the appropriateness of the commonly used value for these heights.

5. Conclusions

In conclusion, the analysis of 63 elevated tank models highlights a critical pattern in the relationship between tank height and the seismic reduction factor (R), emphasizing the need for adjustments in the E.030 standard, particularly for pendulum-type tanks. As tank height increases, the seismic reduction factor decreases, with taller structures exhibiting greater stiffness and sensitivity to horizontal seismic loads. For tanks under 18 m, a higher reduction

factor (R close to 9.6) is applicable; for those between 18 m and 24 m, an intermediate reduction factor ($R = -0.2303X + 11.096$) is recommended; and for tanks over 24 m, a minimum reduction factor ($R = -0.2811X + 10.243$) should be used. Tanks with smaller volumes (10-22.5 m³), which exhibit higher stiffness and lower ductility, require an adjustment to increase R , while larger volume tanks (25-30 m³) with more plastic behavior should benefit from a reduction factor adjustment to reflect their flexibility. For high-rise tanks in the 25-30 m³ range, specific guidelines should account for their greater structural displacement and flexibility, ensuring resilience without compromising stability.

The findings also reveal that taller tanks experience higher ultimate shear forces, ranging from 75.27 tons for a 15 m³ tank (T1_M3) to 178.51 tons for a 25 m³ tank (T6_M7), and significant maximum displacements, reaching 40.66 cm in a 22.5 m³ tank (T3_M6), compared to 5.84 cm in a 27.5 m³ tank (T7_M8). Creep displacement follows a similar trend, with values from 3.47 cm (T7_M4, 17.5 m³) to 12.30 cm (T6_M8, 27.5 m³). Regression analysis revealed low ductility in smaller tanks (10-22.5 m³), resulting in elastic behavior and reduced energy dissipation, while larger tanks (25-30 m³) exhibited desirable plastic behavior, enhancing energy absorption and structural stability. Increased seismic mass in larger volume models contributed to greater flexibility and energy dissipation, aligning with structural dynamics principles.

Future work could focus on analyzing the seismic response of elevated tanks with different types of bases, such as those on softer or rocky soils, which would affect the flexibility and behavior under seismic loads. It is also recommended to incorporate the study of different tank configurations with more varied volumes and heights to broaden the applicability of the results. Limitations of this study include the simplification of boundary conditions and the absence of a complete analysis of soil-structure interaction effects, factors that could influence the accuracy of the results obtained.

REFERENCES

- [1] H. P. Bustamante, "Drinking water, a right denied to half of Loreto" Accessed: Oct. 18, 2024. [Online]. Available: <https://data.larepublica.pe/agua-potable-un-derecho-negado-a-medio-loreto/>
- [2] M. Santos, R. Hausmann, J. Tudela-Pye, J. Lu, and A. Grisanti, "Overcoming Remoteness in the Peruvian Amazonia: A Growth Diagnostic of Loreto," *SSRN Electronic Journal*, Oct. 2022, doi: 10.2139/SSRN.4255155.
- [3] E. Meneses, "Loreto: Water and sanitation works in San Cristóbal with S/ 963,000" Accessed: Oct. 18, 2024. [Online]. Available: <https://peruconstruye.net/2023/08/02/loreto-agua-y-saneamiento-2/>
- [4] P. D. Laureano-Villanueva *et al.*, "Automated system for the control and supply of rainwater in the district of Iquitos," *Proceedings - 2022 International Conference on Mechanical, Automation and Electrical Engineering, CMAEE 2022*, pp. 43–49, 2022, doi: 10.1109/CMAEE58250.2022.00016.
- [5] R. P. del P. Javier, A. M. P. Juan, and José Luis Amado Travezaño, *Standard E.030 Earthquake resistant design*. José Luis Amado Travezaño, 2020, pp. 1–81. Accessed: Oct. 30, 2023. [Online]. Available: <https://drive.google.com/file/d/1W14N6JldWPN8wUZSqWZnUphg6C559bi-/view>
- [6] B. H. Hernandez, "Seismic response of inverted pendulum type elevated tanks," *Sociedad Mexicana de Ingeniería Sísmica A.C.* Accessed: Oct. 18, 2024. [Online]. Available: <https://www.redalyc.org/journal/618/61859035001/html/#B8>
- [7] Puebla, "Newly built water tank collapse kills two people in Puebla | EL PAÍS México." Accessed: Oct. 18, 2024. [Online]. Available: <https://elpais.com/mexico/2022-09-15/el-colapso-de-un-tanque-de-agua-recien-construido-mata-a-dos-personas-en-puebla.html>
- [8] L. M. Adolfo, "Water tank fall leaves 9 injured and damage to 8 homes," *El Universal*. Accessed: Oct. 18, 2024. [Online]. Available: https://es-us.noticias.yahoo.com/ca%C3%ADda-tanque-agua-deja-9-175215238.html?guce_referrer=aHR0cHM6Ly93d3cuZ29vZ2x1LmNvbS8&guce_referrer_sig=AQAAAGVNdKvLAMdtwuTAHqcQBqm3jhN0w6clcoDEDbizfcDdvrH3jsRjpwNBuVyeSivsAD6KwpbfxsJ-QprXnc7ssD4ggny3pFVWw-l-6hQcoPS5wYOLPVtZiLn2obMzEHO9RHkjhqu5MIjWVpPAU1WCTC5Q4iZpTdCFUDc4ueQp1wij&guccounter=1
- [9] ACI Committee 350. and American Concrete Institute., "Code requirements for seismic analysis and design of liquid-containing concrete structures (ACI 350.3-20) and commentary," *American Concrete Institute*, pp. 1–56, 2021.
- [10] E John R. Hayes, & John L. Harris. (2007). Evaluation of the FEMA P-695 Methodology for Quantification of Building Seismic Performance Factors NEHRP Consultants Joint Venture A partnership of the Applied Technology Council and the Consortium of Universities for Research in Earthquake Engineering. National Institute Of Standards and Technology.
- [11] M. Leti, H. Bilgin Online, and H. Bilgin, "Damage potential of near and far-fault ground motions on seismic response of RC buildings designed according to old practices," *Res. Eng. Struct. Mat.*, vol. 8, no. 2, pp. 337–357, 2022, doi: 10.17515/resm2022.392ea0123.
- [12] T. Tafsirojjaman, A. Ur Rahman Dogar, Y. Liu, A. Manalo, and D. P. Thambiratnam, "Performance and design of steel structures reinforced with FRP composites: A state-of-the-art review," *Eng Fail Anal.*, vol. 138, p. 106371, Aug. 2022, doi: 10.1016/J.ENGFAILANAL.2022.106371.
- [13] A. Varvani-Farahani and A. Nayeibi, "Ratcheting in pressurized pipes and equipment: A review on affecting parameters, modelling, safety codes, and challenges," *Fatigue Fract Eng Mater Struct.*, vol. 41, no. 3, pp. 503–538, Mar. 2018, doi: 10.1111/FFE.12775.
- [14] M. Isiet, I. Mišković, and S. Mišković, "Review of

- peridynamic modelling of material failure and damage due to impact,” *Int J Impact Eng*, vol. 147, p. 103740, Jan. 2021, doi: 10.1016/J.IJIMPENG.2020.103740.
- [15] J. jiang Xiong, Y. tao Zhu, C. yang Luo, and Y. sheng Li, “Fatigue-driven failure criterion for progressive damage modelling and fatigue life prediction of composite structures,” *Int J Fatigue*, vol. 145, p. 106110, Apr. 2021, doi: 10.1016/J.IJFATIGUE.2020.106110.
- [16] D. Johnson and M. Sirajuddin, “Behaviour of Elevated Water Tank under Seismic Load-Review,” *International Research Journal of Engineering and Technology*, 2018, Accessed: Oct. 18, 2024. [Online]. Available: www.irjet.net
- [17] N. Workeluel, P. Saha, S. Matiyas, and T. Mohanty, “A comparative study on analysis and design of R. C. C elevated water tank using different country codes,” *Mater Today Proc*, May 2023, doi: 10.1016/J.MATPR.2023.04.486.
- [18] A. Mellati, “Predicting Dynamic Capacity Curve of Elevated Water Tanks: A Pushover Procedure,” *Civil Engineering Journal*, vol. 4, no. 11, pp. 2513–2528, Nov. 2018, doi: 10.28991/cej-03091177.
- [19] N. E. Nasr, M. N. Fayed, G. Hussien, and M. I. El-Far, “EVALUATION OF RESPONSE REDUCTION FACTOR FOR REINFORCED CONCRETE ELEVATED WATER TANKS AND CODES, COMPARATIVE STUDY,” *Journal of Al-Azhar University Engineering Sector*, vol. 17, no. 62, pp. 39–53, 2022.
- [20] J. Amin, K. Gondaliya, and C. Mulchandani, “Assessment of seismic collapse probability of RC shaft supported tank,” *Structures*, vol. 33, pp. 2639–2658, Oct. 2021, doi: 10.1016/J.ISTRUC.2021.06.002.
- [21] O. Ider, H. Hammoum, K. Bouzelha, and A. Aliche, “Evaluation of the Behaviour Coefficient of an Elevated RC Tank,” *Journal of The Institution of Engineers (India): Series A*, vol. 103, no. 1, pp. 1–15, Mar. 2022, doi: 10.1007/S40030-021-00615-Z/METRICS.
- [22] K. N. Patel and J. A. Amin, “Performance-based assessment of response reduction factor of RC-elevated water tank considering soil flexibility: a case study,” *International Journal of Advanced Structural Engineering*, vol. 10, no. 3, pp. 233–247, Sep. 2018, doi: 10.1007/S40091-018-0194-0/FIGURES/8.
- [23] A. V. P. Pandian, K. P. Arunachalam, S. Avudaiappan, S. S. Jasmin, L. M. B. Romero, and P. O. Awoyera, “Modification of response reduction factors of overhead water tanks based on ductility factor,” *Discover Applied Sciences*, vol. 6, no. 4, pp. 1–23, Apr. 2024, doi: 10.1007/S42452-024-05762-Z/FIGURES/16.
- [24] K. N. Patel and J. A. Amin, “Performance-based assessment of response reduction factor of RC-elevated water tank considering soil flexibility: a case study,” *International Journal of Advanced Structural Engineering*, vol. 10, no. 3, pp. 233–247, Sep. 2018, doi: 10.1007/S40091-018-0194-0/FIGURES/8.
- [25] C. Jaiprakash Chitte, S. Charhate, and S. Sangita Mishra, “Seismic Performance of R. C. Elevated Water Storage Tanks,” *Mater Today Proc*, vol. 65, pp. 901–907, Jan. 2022, doi: 10.1016/J.MATPR.2022.03.523.
- [26] A. Eraky, A. Salama, and K. Essam, “Evaluation of the Methodology for Seismic Analysis of Elevated Water Tanks Using Different International Codes of Practice,” Preprint, Sep. 2024, doi: 10.21203/RS.3.RS-4892562/V1.
- [27] N. Workeluel, P. Saha, S. Matiyas, and T. Mohanty, “A comparative study on analysis and design of R. C. C elevated water tank using different country codes,” *Mater Today Proc*, May 2023, doi: 10.1016/J.MATPR.2023.04.486.
- [28] A. Muñoz Pelaez and J. Chavez Angeles, *Standard E.060 Reinforced concrete*, vol. 1. 2020, pp. 1–205. Accessed: Nov. 26, 2023. [Online]. Available: <https://drive.google.com/file/d/19EYUVMgwvm6rDs47GV374avco2yIU5Kz/view>
- [29] S. Chatterji, C. Butenweg, and S. Klinkel, “Integral force-based design approach for the seismic analysis and design of liquid storage tanks,” Preprint, Aug. 2024, doi: 10.21203/RS.3.RS-4874285/V1.
- [30] R. Nascimbene, E. Fagà and M. Moratti, “Seismic Strengthening of Elevated Reinforced Concrete Tanks: Analytical Framework and Validation Techniques,” *Buildings*, vol. 14, no. 7, p. 2254, Jul. 2024, doi: 10.3390/BUILDINGS14072254.
- [31] L. E. Vasquez Munoz, P. Može, and M. Dolšek, “Pushover-based seismic performance assessment of unanchored steel storage tanks with different slenderness ratios,” *Eng Struct*, vol. 305, p. 117742, Apr. 2024, doi: 10.1016/J.ENGSTRUCT.2024.117742.
- [32] J. B. Chouhan and A. M. Gharad, “A review of fluid-structure-soil interaction in elevated water tanks,” *International Journal of Structural Engineering*, vol. 14, no. 4, pp. 356–392, 2024, doi: 10.1504/IJSTRUCTE.2024.142106.
- [33] A. V. P. Pandian, K. P. Arunachalam, S. Avudaiappan, S. S. Jasmin, L. M. B. Romero, and P. O. Awoyera, “Modification of response reduction factors of overhead water tanks based on ductility factor,” *Discover Applied Sciences*, vol. 6, no. 4, pp. 1–23, Apr. 2024, doi: 10.1007/S42452-024-05762-Z/FIGURES/16.
- [34] L. Di Sarno, N. Samanta, K. Dasgupta, and L. of Di Sarno, “Time-Dependent Seismic Performance of the Existing Reinforced Concrete Ductile Flanged Wall-Frame Building: A Numerical Approach.” Accessed: Nov. 27, 2024. [Online]. Available: <https://papers.ssrn.com/abstract=4913251>
- [35] D. Santos, J. Melo, and H. Varum, “Code Requirements for the Seismic Design of Irregular Elevation RC Structures,” *Buildings*, vol. 14, no. 5, p. 1351, May 2024, doi: 10.3390/BUILDINGS14051351.
- [36] “ASCE (American Society of Civil Engineers).” Accessed: Nov. 28, 2024. [Online]. Available: <https://www.asce.org/publications-and-news/codes-and-standards>
- [37] “CEOIS - Centro de Observación para la Ingeniería Sísmica del CISMID/FIC/UNI del CISMID/FIC/UNI.” Accessed: Nov. 28, 2024. [Online]. Available: <https://www.cismid.uni.edu.pe/ceois/red/>
- [38] R. Olivera Perez, T. Julcarima Coca, L. Torpoco Lopez, and M. Laurencio Luna, “Influence of Vertical Geometric Irregularity on the Seismic Response of High-Rise

- Buildings Equipped with Base Isolation System Enhanced Reader,” *Civil Engineering and Architecture*, vol. 12, no. 3A, pp. 2091-2115, 2024, doi: 10.13189/cea.2024.121312.
- [39] J. R. Barik and K. C. Biswal, “Nonlinear seismic analysis of a coupled tank-isolator interactive system using lead rubber bearing,” *Structures*, vol. 65, p. 106647, Jul. 2024, doi: 10.1016/J.ISTRUC.2024.106647.
- [40] M. Pokhrel and M. J. Bandelt, “Plastic hinge behavior and rotation capacity in reinforced ductile concrete flexural members,” *Eng Struct*, vol. 200, p. 109699, Dec. 2019, doi: 10.1016/J.ENGSTRUCT.2019.109699.
- [41] M. G. Vetr, A. Yarmohamadi, and S. Mohammadikish, “Experimental and numerical study on seismic response of RC frames strengthened by shotcrete sandwich panel infills and CFRP strips,” *Structures*, vol. 38, pp. 1244–1256, Apr. 2022, doi: 10.1016/J.ISTRUC.2021.11.052.
- [42] K. A. Harries, “ASCE 41 Seismic Assessment of FRP-Repaired Concrete Columns,” *Journal of Composites for Construction*, vol. 25, no. 2, p. 04021001, Apr. 2021, doi: 10.1061/(ASCE)CC.1943-5614.0001111.
- [43] A. V. Gonchar, V. V. Mishakin, and V. A. Klyushnikov, “The effect of phase transformations induced by cyclic loading on the elastic properties and plastic hysteresis of austenitic stainless steel,” *Int J Fatigue*, vol. 106, pp. 153–158, Jan. 2018, doi: 10.1016/J.IJFATIGUE.2017.10.003.
- [44] K. Marder, K. J. Elwood, C. J. Motter, and G. C. Clifton, “Post-earthquake assessment of moderately damaged reinforced concrete plastic hinges,” *Earthquake Spectra*, vol. 36, no. 1, pp. 299–321, Feb. 2020, doi: 10.1177/8755293019878192.
- [45] K. A. Harries, “ASCE 41 Seismic Assessment of FRP-Repaired Concrete Columns,” *Journal of Composites for Construction*, vol. 25, no. 2, p. 04021001, Apr. 2021, doi: 10.1061/(ASCE)CC.1943-5614.0001111.
- [46] P. A. H. Pham and C. C. Hung, “Assessment of plastic hinge length in reinforced concrete columns,” *Structure and Infrastructure Engineering*, 2023, doi: 10.1080/15732479.2023.2263432.
- [47] K. A. Harries, “ASCE 41 Seismic Assessment of FRP-Repaired Concrete Columns,” *Journal of Composites for Construction*, vol. 25, no. 2, p. 04021001, Apr. 2021, doi: 10.1061/(ASCE)CC.1943-5614.0001111.
- [48] C. Mulchandani and J. Amin, “Assessment of Seismic Response Reduction Factor for RC Shaft Supported Tank,” *Journal of The Institution of Engineers (India): Series A*, vol. 102, no. 1, pp. 75–89, Mar. 2021, doi: 10.1007/S40030-020-00487-9/METRICS.
- [49] K. N. Patel and J. A. Amin, “Performance-based assessment of response reduction factor of RC-elevated water tank considering soil flexibility: a case study,” *International Journal of Advanced Structural Engineering*, vol. 10, no. 3, pp. 233–247, Sep. 2018, doi: 10.1007/S40091-018-0194-0/FIGURES/8.